

Attention-based Class-Conditioned Alignment for Multi-Source Domain Adaptive Object Detection

Atif Belal¹, Akhil Meethal¹, Francisco Perdigon Romero²,
Marco Pedersoli¹, and Eric Granger¹

¹ LIVIA, Dept. of Systems Engineering, ETS Montreal, Canada

² GAIA Montreal, Ericsson Canada

Abstract. Domain adaptation methods for object detection (OD) strive to mitigate the impact of distribution shifts by promoting feature alignment across source and target domains. Multi-source domain adaptation (MSDA) allows leveraging multiple annotated source datasets, and unlabeled target data to improve the accuracy and robustness of the detection model. Most state-of-the-art MSDA methods for OD perform feature alignment in a class-agnostic manner. This is challenging since the objects have unique modal information due to variations in object appearance across domains. A recent prototype-based approach proposed a class-wise alignment, yet it suffers from error accumulation due to noisy pseudo-labels which can negatively affect adaptation with imbalanced data. To overcome these limitations, we propose an attention-based class-conditioned alignment scheme for MSDA that aligns instances of each object category across domains. In particular, an attention module coupled with an adversarial domain classifier allows learning domain-invariant and class-specific instance representations. Experimental results on multiple benchmarking MSDA datasets indicate that our method outperforms the state-of-the-art methods and is robust to class imbalance. Our code is available [here](#).

Keywords: Object Detection · Multi-Source Domain Adaptation.

1 Introduction

Given the recent advancements in deep learning, deep object detectors have shown impressive results on many benchmark problems ranging from closed-world fixed class settings to open-world scenarios [5, 19, 30, 41]. However, their performance typically degrades when there is a domain shift between the training (source) and test (target) data distributions. To address this challenge, several unsupervised domain adaptation (UDA) methods [4, 10, 16, 25] have been proposed to improve OD performance in the presence of a domain shift.

The conventional UDA methods assume that the source data comes only from a single distribution. In real-world scenarios, the source dataset often comes from multiple distributions with considerable domain shifts due to weather, geographic location, and illumination. This setting is referred to as Multi-Source

Domain Adaptation (MSDA) for OD. MSDA is challenging as it requires dealing with discrepancies among sources along with source and target discrepancies. However, having source data from multiple distributions results in enhanced adaptation, increased generalization, and improved robustness against domain shifts [21, 38]. Inspired by the UDA techniques, the typical approach for MSDA involves learning task-specific knowledge from the labeled source datasets, simultaneously trying to make the feature-space domain-invariant that generalizes well to the target domain. Several MSDA methods have been proposed for classification [1, 28, 39], yet MSDA for OD still remains relatively unexplored. This is because in the presence of multiple distribution shifts establishing the trade-off between learning domain-invariant features while preserving task-specific knowledge [15] is challenging when performed both at the image-level and instance level (for OD) compared to only at the image-level (for classification).

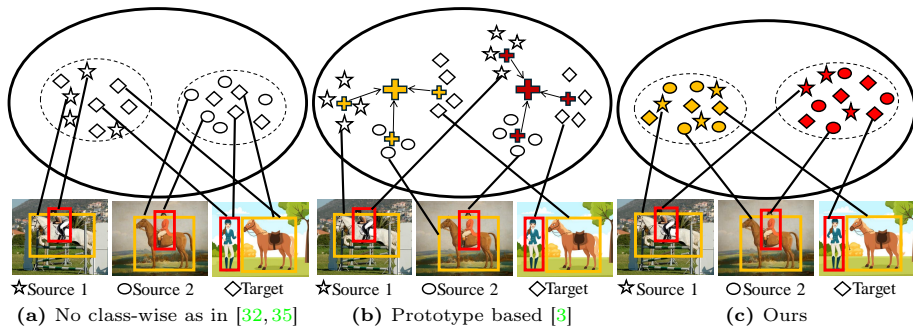


Fig. 1: Comparison of alignment of different MSDA techniques. (a) DMSN and TRKP implement pairwise-alignment of source-target pair without considering class-wise alignment. (b) Prototype based alignment (PMT) learns specific prototypes to represent each class and domain. Then, the same class prototype for different domains are merged in class-conditioned (domain invariant) prototypes. (c) In contrast, our ACIA learns instance-level domain invariant features by conditioning an attention module to attend a given class.

Only three methods have been proposed for MSDA of OD - Divide and Merge Spindle Network (DMSN) [35], Target Relevant Knowledge Preservation (TRKP) [32], and Prototype Mean Teacher (PMT) [3]. DMSN and TRKP focus on pairwise alignment between each source and target pairs as shown in Fig. 1a. This ensures the alignment of each source domain with the target domain. However in a MSDA setting, there are considerable variations in object appearances across domains, so it’s also essential to focus on the class alignment [34]. Else it would lead to class misalignment across domains, which can be observed in Fig. 2a³.

³ As both methods didn’t provide code or trained model, we used our method without instance-level alignment to generate the TSNE.

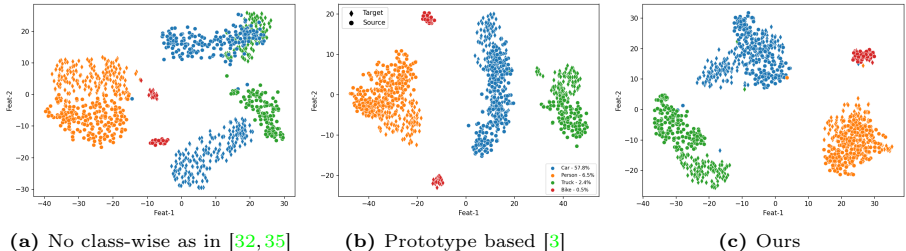


Fig. 2: T-SNE projection of the class distributions on BDD100K of source and target data. **(a)** Projection without class-specific alignment as in DMSN and TRKP. The classes are not aligned between the two domains. **(b)** Prototype-based alignment (PMT) uses prototypes for class alignment. Most classes are well aligned but the bike, as it is underrepresented, is not aligned. **(c)** Our ACIA uses an attention-based adversarial class alignment and manages to align all classes.

Later, PMT proposed a method that uses prototypes for class-conditioned alignment. They use class-specific local and global prototypes to explicitly ensure within-domain and across-domain alignment, as summarized in Fig. 1b. However, this method has a couple of critical limitations. Firstly, they make a strong preassumption that a single prototype can represent the true distribution of a class. But, generally, a class representation is not isotropic, which can be seen in the Fig. 2b. Secondly, they rely on noisy pseudo-labelled target domains to learn the prototypes, resulting in class-misalignment due to error accumulation from the pseudo-labels [6] (we showed that in Tab. 5(right)). This issue is particularly problematic for underrepresented classes, which have fewer samples and can lead to misaligned class representations (empirical result in Tab. 6). This misalignment can be observed in Fig. 2b, where the Bike class (red) is not aligned across the source and target domains. In this scenario, if we calculate the global prototype, it would lie somewhere in the middle of these two distributions, which does not accurately represent the actual class distribution. Consequently, this results in the degradation of the detector’s performance.

This highlights the need for a better class-conditioned instance alignment mechanism in MSDA for OD. In this paper, we propose an Attention-based Class-wise Instance Aligner (ACIA) for MSDA, aiming at efficiently aligning class instances across domains, without relying on prototypical representation. The alignment process of ACIA is illustrated in Fig. 1c where each object category is aligned together across domains. In ACIA, the instances of each ROI-pooled features are infused with the class information by an attention operation. The class information is learned by using a label embedding. To compute the attention output, the query and key values are obtained from ROI-Pooled features, and the key is obtained from label embeddings. The output of the attention is used by adversarial domain discriminator. The gradients are reversed from the output of the instance-level feature extractor forcing those features to be domain-invariant and class-wise aligned at the same time. Our method relies on just a single class embedding to store relative class information for each object category across domains. This allows a simple yet efficient multi-source class-

conditional alignment. The benefits of our class-conditioned aligner can also be observed from Fig. 2, where our ACIA provides better class alignment across domains and robustness to imbalanced data.

Our main contributions are summarized as follows.

- (1) An MSDA method called ACIA is proposed that integrates a conceptually simple class-wise instance alignment scheme. Instance alignment is implemented with an attention mechanism where instances from all domains are aligned to the corresponding class by the attention component.
- (2) The combination of attention and adversarial domain classifier provides instance representations that are simultaneously domain-invariant and class-specific.
- (3) Extensive experiments are conducted on three benchmark MSDA settings to validate the proposed ACIA alignment and ablation of the components. ACIA achieves state-of-the-art performance on all three benchmarks while remaining robust when adapting to imbalanced data. It is the simplest class-conditioned alignment process among the MSDA methods for OD.

2 Literature Review

1. Unsupervised Domain Adaptation. UDA methods aim to learn a model that performs well on the target domain by combining the information from the labeled source data and unlabeled target data. A common approach for UDA is using an adversarial discriminator to generate domain-invariant representation. [8] integrated a GRL-based (reverses the gradient during backpropagation) discriminator at the image and instance level to align the features across domains. Later, [24] showed that strong and weak alignment of high-level and low-level features can improve the performance in UDA. [42] emphasizes the fact that in OD not all parts of the image are equally important. So, they focus on aligning the parts of the images that are more important using clustering and adversarial learning. [40] argues that aligning foreground regions is more important than background regions. They used the output of RPN as an attention map and prototypes for instance-level alignment. [7, 14, 23] tried to mitigate domain shift at the image level. They used Cycle-GAN to convert the source domain to the target domain and minimize the domain shift. These works focus on a single source, however, in this paper, we focus on the MSDA setting where the source data itself has multiple distribution shifts.

2. Multi-Source Domain Adaptation. MSDA methods seek to adapt a model by using samples from multiple labeled source datasets and unlabeled target data. Only three works have been proposed to solve the problem of MSDA in OD - DMSN [35], TRKP [32], and PMT [3]. [35] learns pseudo-subnets for each domain and uses adversarial alignment to align each source subnet with the target. The weight of the target subnet is obtained as the weighted exponential average of the student subnets. [32] proposed an architecture with one detection head for each source domain. These detection heads are trained by using adversarial disentanglement for cross-domain alignment. They also introduced a mining

strategy to weigh each source image based on its relevance to the target domain. Later [3] propose to use class and domain-specific prototypes as a representative of each class per domain. These prototypes are aligned by using contrastive loss to achieve class-conditioned adaptation. Out of the three methods only [3] focuses on class-wise alignment. However, they rely on the assumption that class representations are isotropic and also they suffer from pseudo-label error accumulation [6]. In contrast, our ACIA uses an attention-based adversarial aligner that is immune to pseudo-label error accumulation.

3. Instance-Level Alignment in Domain Adaptation. The instance-level alignment is applied in a DA setting to ensure domain-invariant features at the instance level. [8] uses an adversarial domain classifier at the instance level similar to the image-level discriminator. [13, 33] improved on the work of [8] by giving weight to each ROI-pooled feature during instance-level alignment. This ensures that more importance is given to hard-to-classify features. [42] uses a COGAN to regenerate the ROI-pooled features and later align them using adversarial training. These works align the instance-level features in a class-agnostic way. [29] emphasizes the importance of object category-wise alignment. For this, they used several memory bank prototypes to store class information across domains and they are aligned by using class-specific discriminators. [37] learns a prototype for foreground and background across source and target domain. These prototypes are aligned to produce better predictions on the target domain. [34] learns graph-induced prototypes and proposes a loss to align them. [40] used prototypes and proposed to do instance-level alignment in a class-wise fashion using a prototype-based method. Nevertheless, all these methods rely on learning prototypes for instance-level class alignment in OD, based on the assumption that class representation is isotropic and used pseudo-labels for alignment.

3 Proposed Method

The MSDA setting consists of N source domains S_1, S_2, \dots, S_N and the target domain T . Similar to UDA setting, the object categories across all domains are fixed to a pre-defined set of categories and the number of object categories is K . Each source domain S_j consists of images and corresponding labels, denoted as $S_j = \{(x_i^j, y_i^j)\}_{i=1}^{M_j}$, where $j = 1, 2, \dots, N$, and M_j is the number of images in the source domain j . Here, x_i^j is the i th image from source domain S_j and y_i^j is the set of object labels and corresponding bounding boxes. The target domain T only has images, with no bounding boxes and class labels information. It can be represented as $T = \{x_i^T\}_{i=1}^{M_T}$, where M_T is the number of images in the target domain and x_i^T is the i th image from the target domain.

The training framework of our proposed ACIA is shown in Fig. 3. Our model is based on the Mean-Teacher (MT) framework [10]. The components responsible for image-level and instance-level alignment are integrated into the MT framework. They are the multi-source discriminator and attention-based class-conditioned instance-level discriminator. The MT training process is performed in two stages. First, the student model is trained in a supervised manner on

all source domain data, typically called the burn-in stage in the MT training process [10]. After this step, the teacher model weights are initialized as an exact copy of the student model weights. Then, mutual learning of teacher-student begins on both the labeled source datasets and unlabeled target data. In the case of source datasets, the same supervised training is continued. For the target dataset images, two augmented versions are created for each image, called the weak and strong augmentation. The teacher model receives the weak augmented version and it computes the pseudo-labels. The student model receives the strong augmented version and computes its loss with the pseudo labels provided by the teacher as ground truth. Along with that, the multi-source discriminator and class-conditioned instance-level discriminator are trained for domain-invariant feature generation and class-wise alignment respectively. The weight of the teacher model is the exponential moving Average(EMA) of the weight of the student model. At the time of inference, only the teacher model is used. The rest of the section describes all the loss functions.

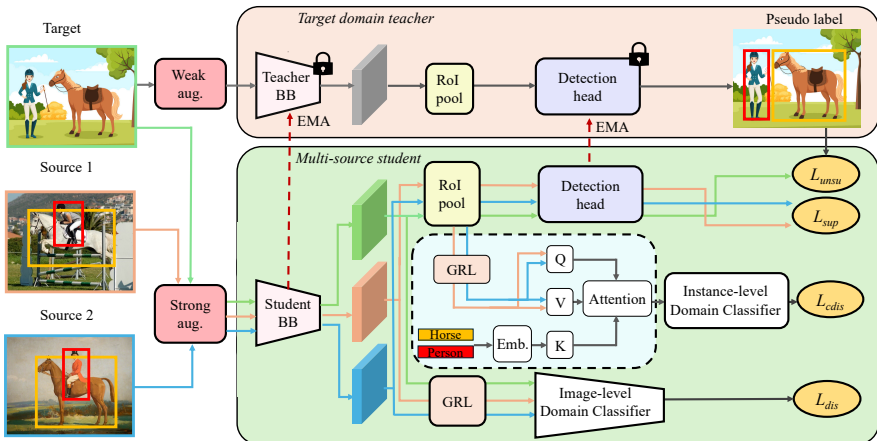


Fig. 3: Overview of the training architecture of our ACIA. The overall architecture is a teacher-student model in which the student learns from multiple sources of data. An image-level classifier is introduced to globally align features, and an instance classifier to align instances in a class-conditional way, through a transformer-based attention block (see white boxes).

1. Source Data Training The source data from all the domains have annotations available. Thus the standard supervised training is applied for the source datasets where the student network weights are updated by backpropagating the detection loss:

$$\mathcal{L}_{\text{sup}} = \sum_{j=1}^N \sum_{i=1}^{M_j} \mathcal{L}_{\text{cls}}(x_i^j, y_i^j) + \mathcal{L}_{\text{reg}}(x_i^j, y_i^j), \quad (1)$$

where \mathcal{L}_{reg} is the smooth-L1 loss [22] used for the bounding box regression and \mathcal{L}_{cls} is the focal loss [17] used for bounding box classification. The source datasets are used in both the training stages, ie, the burn-in and teacher-student mutual learning.

2. Target Data Training Target datasets are used in the training process at the teacher-student mutual learning stage. For every image from the target domain, two augmented versions are generated - strong and weak augmentation. For the strong augmentation, we used color jittering, grayscale, Gaussian blur, and cutout patches. For weak augmentation, image rescaling and horizontal flips are used. The weak augmented image is fed to the teacher model and the output is post-processed to generate pseudo-labels \tilde{y} . The post-processing applied is the confidence thresholding [10]. Let the output of the teacher network for an image x_i be $\hat{y}_i = \{c_i^j, p_i^j, b_i^j\}_{j=1}^D$ where c_i^j, p_i^j, b_i^j are predicted class, probability and box respectively and D is the number of output detections. Then $\tilde{y}_i = \{c_i^j, b_i^j | p_i^j > \theta\}$ where θ is a threshold used for filtering noisy pseudo-labels. The student network then receives the strongly augmented version and computes its loss. The loss function used is the same as eqn. 1, except the pseudo-labels are employed:

$$\mathcal{L}_{\text{unsup}} = \sum_{i=1}^{M_T} \mathcal{L}_{\text{cls}}(x_i, \tilde{y}_i) + \mathcal{L}_{\text{reg}}(x_i, \tilde{y}_i) \quad (2)$$

Once the student weights are updated via backpropagation, the teacher weights are updated as $w_t = \alpha w_t + (1 - \alpha)w_s$ where w_t, w_s are the weights of teacher and student networks respectively and α is a smoothing factor.

3. Image-Level Alignment In the domain adaptation problem, the task-specific knowledge is learned from the source domain. But, for the model to perform well on the target domain, we have to learn a representation that is also domain-invariant. In a UDA setting, this is achieved by attaching a domain discriminator (binary classifier) to the output of the backbone using a gradient-reversal layer (GRL) [16]. This results in a *min-max* optimization game between the backbone and the domain-discriminator, leading to domain-invariant feature representation. Unlike UDA, in MSDA setting the source data comes from various distributions, so we used a multi-class discriminator instead of a binary discriminator. In our work, we used a CNN-based classifier that outputs a domain prediction map from the last feature map of the backbone. The cross-entropy loss is then applied to all pixels of the prediction map and the results are pooled using global average pooling. The training loss of the image-level discriminator can be represented as:

$$\mathcal{L}_{\text{dis}} = -\frac{1}{WH} \sum_{j=1}^{N+1} \sum_{i=1}^{M_j} \sum_{h=1, w=1}^{H, W} d_i^j \log(D(F(x_i^j)_{wh})) \quad (3)$$

Here, W and H are the width and height of the prediction map. $D(F(x_i^j)_{wh})$ is the output of the multi-class discriminator for pixel w, h of the prediction map. D and F represent the discriminator and Feature extractor (the backbone

network in this case) respectively. $d_i \in \{0, 1\}^{N+1}$ whose value is one for the correct domain of the i th image and zero everywhere else.

4. Instance-level Alignment The instance-level alignment is performed in a class-wise fashion in our method. Class-wise alignment helps to align features of objects from the same class regardless of the difference in their visual attributes (such as appearance, scale, orientation, and other characteristics of objects) both within and across domains. Thus even in the presence of class imbalance, underrepresented classes will be focused on ensuring the alignment within and across domains. As shown in fig 2, without class-wise alignment, the separation of class features of the same category across domains is high. PMT [3] is the first MSDA approach in OD that implements class-wise alignment using global and local prototypes. The local prototypes ensured within domain alignment whereas the global prototypes ensured across domain alignment. In contrast to using prototypes for each object category and each domain, we use an efficient attention-based module to ensure class-wise instance alignment.

The instance-level alignment in OD is performed using the region features from each instance. Different from image-level alignment, we have features for a single object category at the instance level. Following the previous approaches, an adversarial discriminator on RoI-Pooled features can be used to perform the instance-level feature alignment. But this alignment process is class-agnostic. If we can perform this adversarial learning in a class-wise fashion, the resulting feature alignment will be class-conditioned. The class information is available for the source domain from the annotations. For the target domain, we can use the filtered pseudo-labels generated by the teacher model. However, the pseudo-labels are noisy, even after filtering. Using them would lead to accumulation error during training from the noises in pseudo-labels [6]. We empirically also found that using the pseudo-labels in class-conditioned alignment harms the model’s performance (see Tab. 5).

To use class information during the alignment process, we create learnable embeddings for each class label. These embeddings can be coupled with region embeddings from the RoI Pool using simple operations like concatenation or multiplication. It is observed that the attention mechanisms are effective at finding relations between two vectors by dynamically focusing on different parts of the sequences [2, 20]. So, we decided to employ an attention-based alignment operation (the results from empirical comparison are available in table 5). For this, two linear projections of the ROI-Pooled features and a linear projection from the label embedding are created. The projections from region embedding are used as query(Q) and value(V) respectively, while the projection from label embedding is used as key(K) for the attention block (see Fig. 3). The attention block uses a multi-head attention as proposed in the original paper [27] which can be expressed as:

$$\text{Attention}(Q, K, V) = \text{softmax} \left(\frac{QK^T}{\sqrt{d_K}} \right) V \quad (4)$$

where d_K is the size of the key K . The dot-product of K and Q allows our model to learn the relation between the object features and class labels based on object

category and image domain. Later, the dot-product of this with V , allows our model to learn which part of the object feature to focus on for class-conditioned adaptation. We also combine multiple single-head attention to get multi-head attention. This allows our method to learn multiple such relations. At the end of the attention block, a classification head is used to predict the domain of the input instance. The instance aligner is trained with the cross-entropy loss:

$$\mathcal{L}_{\text{cdis}} = - \sum_{j=1}^N \sum_{i=1}^{M_i} \frac{1}{Z_i^j} \sum_{r=1}^{Z_i^j} d_i^j \log(D(R(F(z_{i,r}^j)))) , \quad (5)$$

where D , R , and F represent the Discriminator, ROI-Pooling, and Feature extractor of the student model; Z_i^j is the number of Ground Truth(GT) instances in i th image from domain j , and $z_{i,r}^j$ is the r th GT box on i th image from domain j . The target of the discriminator, $d_i \in \{0, 1\}^N$, is the domain label for each GT box as in Eq. (3). Note that d_i is of length N because we are not considering (pseudo) GTs from the target image.

Final Training Objective: After starting the student-teacher mutual learning all the losses discussed above are combined and used for training the student model. So, the final training loss for the student model would be:

$$\mathcal{L} = \mathcal{L}_{\text{sup}} + \alpha \mathcal{L}_{\text{unsup}} + \beta \mathcal{L}_{\text{dis}} + \gamma \mathcal{L}_{\text{cdis}} , \quad (6)$$

where α , β , and γ are hyper-parameters for weighing each losses. The teacher model is updated as an EMA of the student model at each iteration.

4 Results and Discussion

4.1 Experimental Methodology

1. Implementation Details - In our experiments, we follow the same settings as [3, 32, 35]. In all experiments, Faster-RCNN [22] with Imagenet pretrained VGG-16 backbone is used as the detector. Images are resized such that the shorter side of the image is 600 while maintaining the image ratios, following the ROI-alignment [12] based implementation of Faster-RCNN. For the hyper-parameters, we set α , β and γ to 1, 0.1 and 0.3, respectively. The pseudo-label threshold was set to 0.7 for all the experiments. As mentioned in 3, our training is two-staged. We trained our model for 15 epochs in both the settings. We set the weight smoothing coefficient for EMA of teacher mode to 0.9996. All experiments were done on 4 A100 GPUs, with batch size and learning rate of 8 and 0.2 respectively. We implemented our method using Pytorch.

2. Baseline Methods - We compared our results against four settings: 1 - Lower Bound - Supervised training on the merged source data. 2 - UDA - Source domains are blended and the UDA method is used. 3 - MSDA - SOTA MSDA methods fall into this category. 4 - Upper Bound - We have 3 upper bounds: Target Only - Supervised training on target data, All-Combined - Supervise

Setting	Src.1	# Img.	Src.2	# Img.	Src.3	# Img.	Target	# Img.
Cross-time	Day	36,728	Night	27,971	-	-	Dawn	5,027
Cross-camera	Cityscapes	2,831	Kitty	6,684	-	-	Day	36,728
Mixed Domain	Cityscapes	2,975	COCO	71,745	Synscapes	25,000	Day	36,728

Table 1: Summary of the different MSDA settings used in our study.

training on target and source combined, Fine-Tuning - Trained on source domain, then fine-tuned on the target domain.

3. Datasets and Adaptation Setting For our experiments we use 5 different datasets with various objects and different domains and capturing conditions: BDD100K [36], Cityscapes [9], KITTI [11], MS COCO [18] and Synscapes [31]. The MSDA problem settings used in the empirical study are summarized in Tab. 1. For each setting, the source and target domains used are listed as well.

4.2 Results

1. Cross-time Adaptation - Daytime and Night subsets of BDD100K dataset are used as source domain, while the Dusk/Dawn subset of BDD100K is used as target domain. In this setting the images are captured at different times. This causes a domain shift due to variation in illumination.

We reported the result of our method, against other baseline in Tab. 2. It can be observed that the DAOD methods outperforms the Lower Bound. But, there is a slight decrease in performance when the Night domain is added to the Daytime domain. This is because the UDA Blending methods did not consider the domain shift among the source domains, resulting in a degradation of performance. This emphasizes the importance of research on the MSDA methods. Our method beats the previous state of art MSDA method [3] by 2.6 mAP. Also, our method outperforms Target-Only and All-Combined Upper Bound Settings. The poor performance of the Target Only setting is due to fewer samples in the target domain compared to source domains.

2. Cross-camera Adaptation- Cityscapes and Kitty datasets are used as source domains, while the Daytime subset of BDD100K is used as the target domain. In this setting the images are captured using different cameras. This causes a domain shift due to variations in the camera’s resolution and view-point. In this setting, the training and evaluation is done only on the car object category (the only overlapping class across the domains).

The AP on car compared against the baselines is reported in Tab. 2. The general variation of performance in this setting is similar to Sec. 4.2 setting. Our proposed method is able to outperform the previous method by 0.4%. Our result is also very close to the target-only upper-bound. In this setting there is only one object category, thus the class-conditioning has no impact in instance alignment. As shown in the ablation studies, the class-conditioning during instance alignment is crucial for the performance improvement.

3. Extension to Mixed Domain Adaptation - MS COCO, Cityscapes, and Synscapes datasets are used as source domain. While, the Daytime subset of BDD100K is used as target domain. In the real-world data the domain shift

Setting	Method	D	N	D+N	C	K	C+K
Lower Bound	Source Only	30.4	25.0	28.9	44.6	28.6	43.2
UDA	Strong-Weak [26]	31.4	26.9	29.9	45.5	29.6	41.9
	Graph Prototype [4]	31.8	27.6	30.6	-	-	-
	Cat. Regularization [33]	31.2	28.4	30.2	46.5	30.8	43.6
	UMT [10]	33.8	21.6	33.5	47.5	35.4	47.0
	Adaptive Teacher [16]	34.9	27.8	34.6	49.8	40.1	48.4
MSDA	MDAN [38]	-	-	27.6	-	-	43.2
	M ³ SDA [21]	-	-	26.5	-	-	44.1
	DMSN [35]	-	-	35.0	-	-	49.2
	TRKP [32]	-	-	39.8	-	-	58.4
	PMT [3]	-	-	45.3	-	-	58.7
	ACIA (Ours)	-	-	47.9	-	-	59.1
Upper Bound	Target-Only	-	-	26.6	-	-	60.2
	All-Combined	-	-	45.6	-	-	69.7
	Fine-Tuning	-	-	50.9	-	-	72.1

Table 2: Detection mAP of our method compared against the baselines in the cross-time (left) and cross-camera (right) setting. Source domains are daytime (D) and night (N) subsets and the target is *Dusk/Dawn* subset of BDD100K in cross-time setting. And, for the cross-camera setting source domains are Cityscapes (C) and Kitty (K) and the target is *Daytime* subset of BDD100K.

is not limited to a single factor. So, in this setting domain shift occurs due to multiple and variable reasons. Also, in this setting, we have three source domains, instead of two. These reasons make this setting challenging and very close to practical setting.

The empirical results from this setting is presented in Tab. 3. In this setting the Lower Bound is performing better than the UDA Blending baseline. We hypothesize this is due to large domain shift among domains so blending all the source domain as one and using UDA is resulting in performance degradation. This highlights the difficulty of this setting. When compared with the previous MSDA methods, our method is outperforming them. When Cityscapes and MS COCO are used as source domain, we’re outperforming the previous SOTA result by 2.3 mAP. When Synscapes is also added to the source domain this number rises to 2.6 mAP. This shows that our method continues to improve the performing when source domain are added. Our method is also outperforming the Target Only Upper Bound.

4.3 Ablation Studies

Unless mentioned, all the ablation studies are performed on the cross-time adaptation setting as in [3,35]. The impact of the components performing image-level and instance-level feature alignment is analyzed along with other possible design choices for class-conditioned instance alignment.

1. Impact of the adaptation components - First, we analyzed the impact of the individual components of our proposed method. These components include image-level discriminator and instance-level discriminator. To better understand

Setting	Method	C	C+M	C+M+S
Lower Bound	Source Only	23.4	29.7	30.9
UDA	UMT [10]	-	18.5	25.1
	Adaptive Teach. [16]	-	22.9	29.6
MSDA	TRKP [32]	-	35.3	37.1
	PMT [3]	-	38.7	39.7
	ACIA (Ours)	-	41.0	42.3
Upper Bound	Target-Only	-	-	38.6
	All-Combined	-	47.1	48.2
	Fine-Tuning	-	49.2	52.5

Table 3: mAP on 7 object categories of our method compared against baselines in the mixed setting. Source domains are Cityscapes(C), MS COCO(M), and Synscapes(S) datasets while the *Daytime* domain of BDD100K is target domain.

Image-LA	Instance-LA w/o class-embed.	Instance-LA w/ class-embed.	AP ₅₀
			31.7
✓			41.9
✓	✓		45.3
✓		✓	47.9

Table 4: Impact of individual components our ACIA method. Image-LA: Image-Level Alignment, Instance-LA: Instance-Level Alignment.

the importance of class conditioning in the instance alignment, we further examined the instance classifier with and without class-wise attention. The results are reported in Tab. 4. It can be observed that just by adding the image-level discriminator, the performance improved by a huge margin. Furthermore, by adding the instance-level discriminator (without class-embedding) the performance of the model increased by 3.4% showing the importance of instance-level alignment. The performance is further boosted by integrating the class-information into the instance-level alignment.

2. Design choices for class-wise instance alignment - The instance-level alignment component can be designed in different ways. Apart from the attention-based method, class information can be incorporated to instances by concatenation and multiplication. Tab. 5(left) reports the variation in performance with different design choice. It is clear that attention is the superior design choice. We believe this is because we’re learning just one class-embedding layer across every domain. When we’re merging the class-information to the ROI-Pool features, attention can learn what information is more important for a particular domain in a better way than multiplication and concatenation. This is because of the design of the attention layer, allowing it to learn complex relations [27].

3. Impact of target domain on class-wise alignment - Instance-level alignment differs from image-level alignment in that it focuses solely on the foreground region of the image. In this section, we investigate the impact of employing or omitting the target image in instance-level alignment. As reported in Tab. 5 (right), utilizing target data in both scenarios leads to a decline in detector performance. In a DA scenario, the target data lack labels, making it challenging

Merging	D+N	Setting	With Target	Without Target
Concatenation	46.3	Cross-Time	43.3	47.9
Multiplication	46.8	Mixed	37.9	41.0
Attention	47.9			

Table 5: (left) Different design choices for integrating class information in instance alignment; (right) Detection performance degrades when target domain is used in the instance alignment process.

to distinguish between foreground regions and object categories. One approach to address this challenge is by employing pseudo-labels; however, they often introduce noise and degrade performance. Nonetheless, in MSDA, the availability of multiple source domains enables us to choose which domains to align at the instance level. Hence, our work focuses on aligning solely the source domains.

4. Detection Visualization In Fig. 4 we present the visualization of detections on BDD100k cross-time for the three multi-source adaptation approaches presented in the paper: no class-wise adaptation, prototype-based class-conditional adaptation and our attention-based class-conditional adaptation.

5. Level of Imbalance In Tab. 6 we compare our method against PMT for different levels of imbalance. As expected, when the dataset is balanced the two methods perform similarly. However, when the level of imbalance increases, our method obtains much better mAP. This shows that the error accumulation from the pseudo-labels is more problematic in the case of imbalanced datasets. Our class-conditioned attention model solves that issue, as it uses the same model for all classes and therefore can better deal with high levels of imbalance.

Method	Bike	Bus	Car	Motor	Person	Rider	Light	Sign	Truck	mAP
<i>Mostly Balanced</i>	25.0	50.0		10.0		15.0				
PMT	43.8	52.3	-	28.0	-	34.4	-	-	-	39.6
Ours	45.8	48.9	-	30.7	-	31.0	-	-	-	39.1
<i>Slightly Imbalanced</i>	4.6	9.2		1.8	59.6	2.8			22.0	
PMT	42.1	52.7	-	25.1	43.1	34.0	-	-	50.5	41.2
Ours	44.3	54.2	-	25.3	45.3	40.6	-	-	50.4	43.4
<i>Mostly Imbalanced</i>	1.2	2.4		0.5	15.4	0.7	32.8	42.3	5.7	
PMT	49.2	56.2	-	29.6	49.9	32.0	43.2	55.8	55.3	46.4
Ours	52.1	59.2	-	29.2	53.1	36.1	46.2	58.1	57.1	48.9
<i>Highly Imbalanced</i>	0.5	1	57.8	0.2	6.5	0.3	13.4	17.8	2.4	
PMT	55.3	59.8	67.6	29.9	47.6	32.7	46.3	56.0	57.7	50.3
Ours	56.1	61.0	69.2	31.9	51.8	39.8	49.2	59.0	61.0	53.2

Table 6: Detection results per-class on cross-time setting for PMT and our method with different levels of imbalance. The dataset is quite imbalanced. To create a more balanced dataset we reduced the number of classes by removing those that are creating the imbalance. For each level of imbalance, we report the relative importance of each class in percentage.



Fig. 4: Examples of ODs on BDD100k cross-time setting, with different types of instance-level adaptation. (a) ODs with a multi-source adaptation without instance level class-conditional adaptation as in [32, 35]. (b) ODs with the prototype-based class-conditional adaptation [3]. (c) ODs with our ACAI approach.

5 Conclusion

Recent studies in UDA have observed that doing instance alignment in a class-conditioned fashion has impressive results. However, a comprehensive study on class-conditioning in MSDA for OD to understand its impact and contribution for instance alignment is missing in existing works. Also, the existing techniques for class-conditioning have several limitations that can lead to misalignment of instances. We empirically observed this misalignment in the case of underrepresented classes. Our work is addressing this research gap with the goal of developing an efficient class-conditioned instance alignment for MSDA. We propose an attention-based class-conditioning scheme for instance alignment where attention operation between region embeddings and label embeddings coupled with an adversarial domain classifier promotes the domain-invariance of object instances in a class-conditioned manner. The resulting instance-alignment scheme obtained state-of-the-art results on popular MSDA benchmarks while being robust to class imbalance.

References

1. Amosy, O., Chechik, G.: Coupled training for multi-source domain adaptation. In: IEEE/CVF Winter Conference on Applications of Computer Vision (WACV) (2022) **2**
2. Bahdanau, D., Cho, K., Bengio, Y.: Neural machine translation by jointly learning to align and translate (2016) **8**
3. Belal, A., Meethal, A., Romero, F.P., Pedersoli, M., Granger, E.: Multi-source domain adaptation for object detection with prototype-based mean teacher. In: IEEE/CVF Winter Conference on Applications of Computer Vision (WACV). pp. 1277–1286 (January 2024) **2, 3, 4, 5, 8, 9, 10, 11, 12, 14, 20, 21**
4. Cai, Q., Pan, Y., Ngo, C.W., Tian, X., Duan, L., Yao, T.: Exploring object relation in mean teacher for cross-domain detection (2019). <https://doi.org/10.48550/ARXIV.1904.11245>, <https://arxiv.org/abs/1904.11245> **1, 11, 20**
5. Carion, N., Massa, F., Synnaeve, G., Usunier, N., Kirillov, A., Zagoruyko, S.: End-to-end object detection with transformers (2020) **1**
6. Chen, C., Xie, W., Huang, W., Rong, Y., Ding, X., Huang, Y., Xu, T., Huang, J.: Progressive feature alignment for unsupervised domain adaptation (2019) **3, 5, 8**
7. Chen, C., Zheng, Z., Ding, X., Huang, Y., Dou, Q.: Harmonizing transferability and discriminability for adapting object detectors (2020) **4**
8. Chen, Y., Li, W., Sakaridis, C., Dai, D., Van Gool, L.: Domain adaptive faster r-cnn for object detection in the wild (2018). <https://doi.org/10.48550/ARXIV.1803.03243>, <https://arxiv.org/abs/1803.03243> **4, 5**
9. Cordts, M., Omran, M., Ramos, S., Rehfeld, T., Enzweiler, M., Benenson, R., Franke, U., Roth, S., Schiele, B.: The cityscapes dataset for semantic urban scene understanding (2016) **10, 18**
10. Deng, J., Li, W., Chen, Y., Duan, L.: Unbiased mean teacher for cross-domain object detection (2021) **1, 5, 6, 7, 11, 12, 20**
11. Geiger, A., Lenz, P., Urtasun, R.: Are we ready for autonomous driving? the kitti vision benchmark suite. In: 2012 IEEE Conference on Computer Vision and Pattern Recognition. pp. 3354–3361 (2012). <https://doi.org/10.1109/CVPR.2012.6248074> **10, 18**
12. He, K., Gkioxari, G., Dollár, P., Girshick, R.: Mask r-cnn (2018) **9**
13. He, Z., Zhang, L.: Multi-adversarial faster-rcnn for unrestricted object detection (2019) **5**
14. Hsu, H.K., Yao, C.H., Tsai, Y.H., Hung, W.C., Tseng, H.Y., Singh, M., Yang, M.H.: Progressive domain adaptation for object detection (2019). <https://doi.org/10.48550/ARXIV.1910.11319>, <https://arxiv.org/abs/1910.11319> **4**
15. Kundu, J.N., Kulkarni, A.R., Bhamri, S., Mehta, D., Kulkarni, S.A., Jampani, V., Radhakrishnan, V.B.: Balancing discriminability and transferability for source-free domain adaptation. In: International Conference on Machine Learning (2022) **2**
16. Li, Y.J., Dai, X., Ma, C.Y., Liu, Y.C., Chen, K., Wu, B., He, Z., Kitani, K., Vajda, P.: Cross-domain adaptive teacher for object detection (2021). <https://doi.org/10.48550/ARXIV.2111.13216>, <https://arxiv.org/abs/2111.13216> **1, 7, 11, 12, 18, 20**
17. Lin, T.Y., Goyal, P., Girshick, R., He, K., Dollár, P.: Focal loss for dense object detection. IEEE Transactions on Pattern Analysis and Machine Intelligence (2020) **7**
18. Lin, T.Y., Maire, M., Belongie, S., Bourdev, L., Girshick, R., Hays, J., Perona, P., Ramanan, D., Zitnick, C.L., Dollár, P.: Microsoft coco: Common objects in context (2015) **10, 18**

19. Liu, S., Zeng, Z., Ren, T., Li, F., Zhang, H., Yang, J., Li, C., Yang, J., Su, H., Zhu, J., et al.: Grounding dino: Marrying dino with grounded pre-training for open-set object detection. arXiv preprint arXiv:2303.05499 (2023) **1**
20. Luong, T., Pham, H., Manning, C.D.: Effective approaches to attention-based neural machine translation. In: Màrquez, L., Callison-Burch, C., Su, J. (eds.) Proceedings of the 2015 Conference on Empirical Methods in Natural Language Processing. pp. 1412–1421. Association for Computational Linguistics, Lisbon, Portugal (Sep 2015). <https://doi.org/10.18653/v1/D15-1166>, <https://aclanthology.org/D15-1166> **8**
21. Peng, X., Bai, Q., Xia, X., Huang, Z., Saenko, K., Wang, B.: Moment matching for multi-source domain adaptation (2019) **2, 11, 20**
22. Ren, S., He, K., Girshick, R., Sun, J.: Faster r-cnn: Towards real-time object detection with region proposal networks (2016) **7, 9**
23. Rodriguez, A.L., a, Mikolajczyk, K.: Domain adaptation for object detection via style consistency (2019). <https://doi.org/10.48550/ARXIV.1911.10033>, <https://arxiv.org/abs/1911.10033> **4**
24. Saito, K., Ushiku, Y., Harada, T., Saenko, K.: Strong-weak distribution alignment for adaptive object detection (2018). <https://doi.org/10.48550/ARXIV.1812.04798>, <https://arxiv.org/abs/1812.04798> **4**
25. Saito, K., Ushiku, Y., Harada, T., Saenko, K.: Strong-weak distribution alignment for adaptive object detection. In: CVPR (2019) **1, 18**
26. Saito, K., Ushiku, Y., Harada, T., Saenko, K.: Strong-weak distribution alignment for adaptive object detection. In: IEEE/CVF Conference on Computer Vision and Pattern Recognition (CVPR) (2019) **11, 20**
27. Vaswani, A., Shazeer, N., Parmar, N., Uszkoreit, J., Jones, L., Gomez, A.N., Kaiser, L., Polosukhin, I.: Attention is all you need (2023) **8, 12**
28. Venkat, N., Kundu, J.N., Singh, D.K., Revanur, A., Babu, R.V.: Your classifier can secretly suffice multi-source domain adaptation. In: Advances in Neural Information Processing Systems (NeurIPS) (2020) **2**
29. VS, V., Gupta, V., Oza, P., Sindagi, V.A., Patel, V.M.: Mega-cda: Memory guided attention for category-aware unsupervised domain adaptive object detection (2021) **5**
30. Wang, C.Y., Bochkovskiy, A., Liao, H.Y.M.: YOLOv7: Trainable bag-of-freebies sets new state-of-the-art for real-time object detectors. In: IEEE/CVF Conference on Computer Vision and Pattern Recognition (CVPR) (2023) **1**
31. Wrenninge, M., Unger, J.: Synscapes: A photorealistic synthetic dataset for street scene parsing (2018) **10, 18**
32. Wu, J., Chen, J., He, M., Wang, Y., Li, B., Ma, B., Gan, W., Wu, W., Wang, Y., Huang, D.: Target-relevant knowledge preservation for multi-source domain adaptive object detection (2022). <https://doi.org/10.48550/ARXIV.2204.07964>, <https://arxiv.org/abs/2204.07964> **2, 3, 4, 9, 11, 12, 14, 20, 21**
33. Xu, C.D., Zhao, X.R., Jin, X., Wei, X.S.: Exploring categorical regularization for domain adaptive object detection (2020) **5, 11, 20**
34. Xu, M., Wang, H., Ni, B., Tian, Q., Zhang, W.: Cross-domain detection via graph-induced prototype alignment (2020) **2, 5**
35. Yao, X., Zhao, S., Xu, P., Yang, J.: Multi-source domain adaptation for object detection (2021). <https://doi.org/10.48550/ARXIV.2106.15793>, <https://arxiv.org/abs/2106.15793> **2, 3, 4, 9, 11, 14, 20, 21**
36. Yu, F., Chen, H., Wang, X., Xian, W., Chen, Y., Liu, F., Madhavan, V., Darrell, T.: Bdd100k: A diverse driving dataset for heterogeneous multitask learning (2020) **10, 18**

37. Zhang, Y., Wang, Z., Mao, Y.: Rpn prototype alignment for domain adaptive object detector. In: IEEE/CVF Conference on Computer Vision and Pattern Recognition (CVPR). pp. 12425–12434 (June 2021) [5](#)
38. Zhao, H., Zhang, S., Wu, G., Moura, J.M.F., Costeira, J.P., Gordon, G.J.: Adversarial multiple source domain adaptation. In: Advances in Neural Information Processing Systems (2018) [2](#), [11](#), [20](#)
39. Zhao, H., Zhang, S., Wu, G., Moura, J.M.F., Costeira, J.P., Gordon, G.J.: Adversarial multiple source domain adaptation. In: Bengio, S., Wallach, H., Larochelle, H., Grauman, K., Cesa-Bianchi, N., Garnett, R. (eds.) Advances in Neural Information Processing Systems. Curran Associates, Inc. (2018) [2](#)
40. Zheng, Y., Huang, D., Liu, S., Wang, Y.: Cross-domain object detection through coarse-to-fine feature adaptation (2020) [4](#), [5](#)
41. Zhou, X., Girdhar, R., Joulin, A., Krähenbühl, P., Misra, I.: Detecting twenty-thousand classes using image-level supervision. In: ECCV (2022) [1](#)
42. Zhu, X., Pang, J., Yang, C., Shi, J., Lin, D.: Adapting object detectors via selective cross-domain alignment. In: IEEE/CVF Conference on Computer Vision and Pattern Recognition (CVPR) (June 2019) [4](#), [5](#)

6 Appendix

6.1 Datasets

There are five datasets used to create the multi-source domain adaptation settings in our study. These datasets are listed below:

1. **BDD100k** - The BDD100K [36] is a large-scale diverse driving dataset. It contains 70,000 training and 10,000 testing images captured across various times, like Daytime, Night, and Dusk/Dawn. This variation makes it a good choice for DA problem.
2. **Cityscapes** - Cityscapes [9] is an autonomous driving research dataset, with images captured from urban street scenes. It contains 2,975 training and 500 testing images.
3. **Kitty** - The KITTI [11] dataset is a driving dataset, that comprises a collection of images and associated sensor data captured from a moving vehicle in urban environments. It consists of 7,481 training images RGB images.
4. **MS COCO** - MS COCO [18] is one of the most widely-used benchmark dataset in computer vision. It is a complex dataset having large scale and appearance variations for the instances. It has around 330,000 images containing 80 object categories.
5. **Synscapes** - Synscapes [31] is a synthetic autonomous driving dataset, that gives more variability for testing our method. It consists of 25,000 training images.

6.2 Effect of Class-Alignment in UDA methods

In this subsection we show the effect of class-wise alignment on UDA methods [16, 25]. Tab. 7 shows the results. We studied three different cases; 1. No class alignment - we used their proposed method only. 2. Class-Alignment with target domain - here we incorporated our class alignment component with their method, aligning the source domains and the target domain. 3. Class-Alignment without target domain - our class alignment component with their method, but this time only the source domains are considered. The results clearly show that our class alignment is effective with both methods. Thus we can conclude that the proposed class-conditional alignment is effective for both UDA and MSDA methods. It can be also observed that, similar to our method, removing target data for the instance-level alignment further enhances the model performance.

Method	No Class Align.	Class-Align. w/ Target	Class-Align. w/o Target
Strong-Weak [25]	29.9	33.7	34.2
Adaptive Teacher [16]	34.6	36.8	37.6

Table 7: Importance of Class-alignment in UDA methods. The proposed attention-based class-conditioned aligner is effective for UDA methods as well.

6.3 Architecture of the Discriminator Networks

We use two domain classifiers as the discriminator networks for adversarial training: an image-level domain classifier and an instance-level domain classifier. Their architecture is summarized in Fig. 5. The image-level domain classifier receives its input from the final layer of the backbone network used for feature extraction. This classifier is fully convolutional with a final $N+1$ class prediction layer (corresponds to number of source domains plus the target domain). The instance-level classifier receives its input from the attention layer. This classifier consists of only linear layers with a final N -way prediction layer (the target domain is not used here because the GT boxes from the target domain are not available).

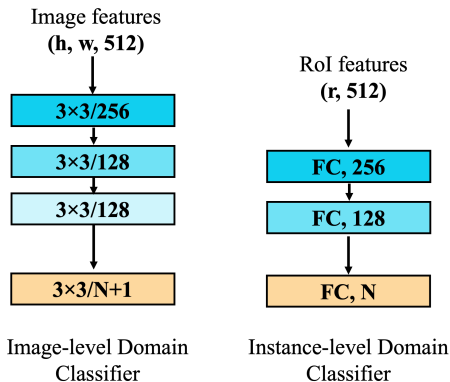


Fig. 5: Detailed architecture of the networks used for image-level and instance-level domain classifiers. The activation functions used in image-level and instance-level classifiers are leaky ReLU and GELU respectively. Additionally, Layernorm is used in the instance-level domain classifier. (r = no of GT boxes in the image, h,w = height and width of the feature map, FC = Fully connected layer)

6.4 Class-wise AP

We also report the detailed class-wise AP of ACIA on the Cross-time and Mixed Adaptation settings in Tab. 8 and Tab. 9 respectively. Note that, for the Cross-camera Adaptation settings, there is only one class, so this is not applicable.

In both settings, our method outperforms the others for all classes. The class-wise AP shows improvement both in the majority and minority classes as well - eg: car (majority) and traffic sign (minority) in the cross-time settings. In the mixed adaptation settings, we outperform others for all the classes, in both the case of two and three source domains.

6.5 More Detection Visualization

In Fig. 6 we present more visualization of the detections on BDD100k cross-time for the three multi-source adaptation approaches presented in the paper:

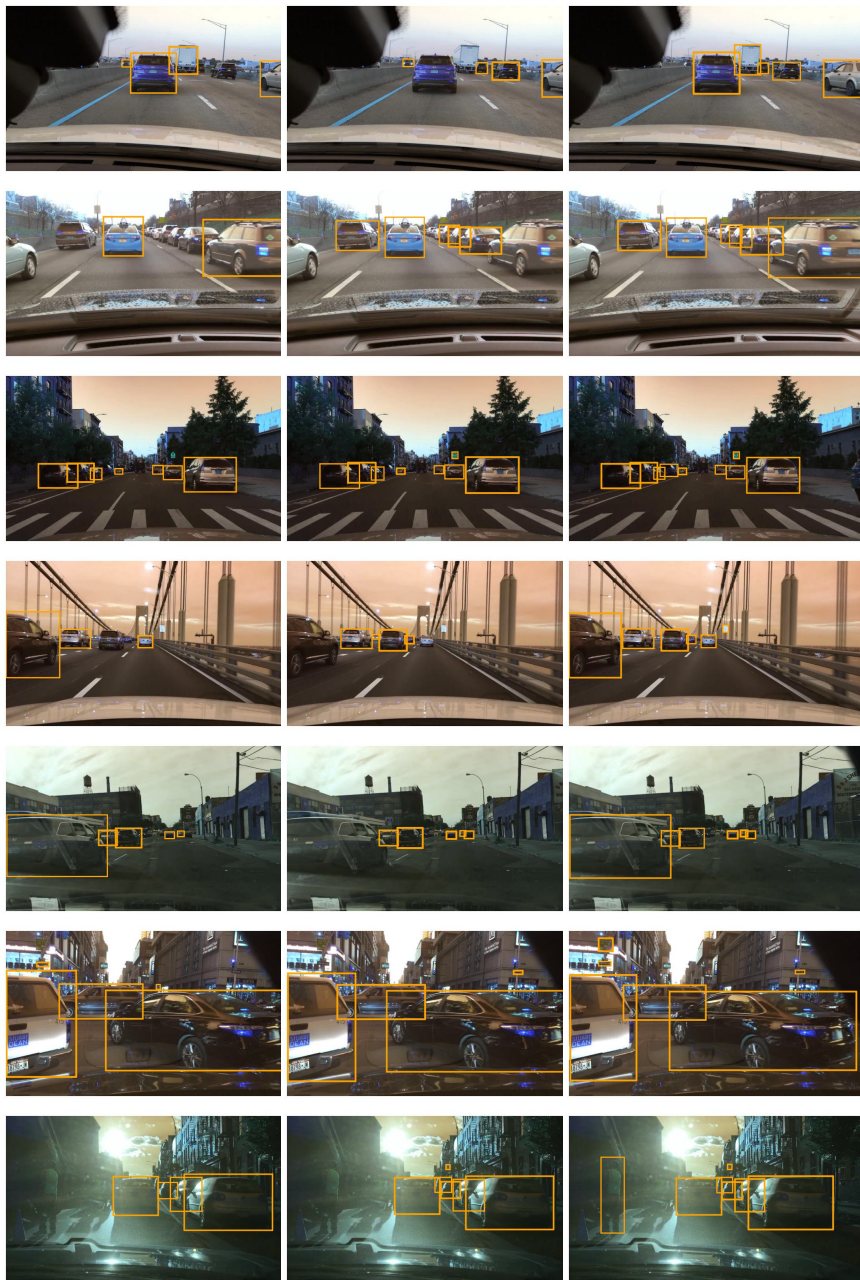
no class-wise adaptation (similar to [32, 35]), prototype-based class-conditional adaptation [3] and our attention-based class-conditional adaptation. From the visualizations, it can be observed that our method is performing better detection compared to the other approaches highlighting the impact of an efficient class-conditioned alignment.

Setting	Source	Method	Bike	Bus	Car	Motor	Person	Rider	Light	Sign	Train	Truck	mAP
Lower Bound	D	Source Only	35.1	51.7	52.6	9.9	31.9	17.8	21.6	36.3	-	47.1	30.4
	N		27.9	32.5	49.4	15.0	28.7	21.8	14.0	30.5	-	30.7	25.0
	D+N		31.5	46.9	52.9	8.4	29.5	21.6	21.7	34.3	-	42.2	28.9
UDA	D+N	Strong-Weak [26]	29.7	50.0	52.9	11.0	31.4	21.1	23.3	35.1	-	44.9	29.9
		Graph Prototype [4]	31.7	48.8	53.9	20.8	32.0	21.6	20.5	33.7	-	43.1	30.6
		Cat. Regularization [33]	25.3	51.3	52.1	17.0	33.4	18.9	20.7	34.8	-	47.9	30.2
		UMT [10]	42.3	48.1	56.4	13.5	35.3	26.9	31.1	41.7	-	40.1	33.5
		Adaptive Teacher [16]	43.1	48.9	56.9	14.7	36.0	27.1	32.7	43.8	-	42.7	34.6
MSDA	D+N	MDAN [38]	37.1	29.9	52.8	15.8	35.1	21.6	24.7	38.8	-	20.1	27.6
		M ³ SDA [21]	36.9	25.9	51.9	15.1	35.7	20.5	24.7	38.1	-	15.9	26.5
		DMSN [35]	36.5	54.3	55.5	20.4	36.9	27.7	26.4	41.6	-	50.8	35.0
		TRKP [32]	48.4	56.3	61.4	22.5	41.5	27.0	41.1	47.9	-	51.9	39.8
		PMT [3]	55.3	59.8	67.6	29.9	47.6	32.7	46.3	56.0	-	57.7	45.3
		ACIA(ours)	56.1	61.0	69.2	31.9	51.8	39.8	49.2	59.0	-	61.0	47.9
Upper Bound	D+N	Target Only	27.2	39.6	51.9	12.7	29.0	15.2	20.0	33.1	-	37.5	26.6
		All-Combined	56.4	59.9	67.3	30.8	47.9	33.9	47.2	57.8	-	54.8	45.3
		Fine-Tuning	63.3	68.1	72.5	39.3	52.2	37.2	54.1	63.1	-	59.1	50.9

Table 8: Class-wise AP of ACIA compared against the baseline lower bound, UDA, MSDA, and upper bound methods in the cross-time settings. Source domains are daytime (D) and night (N) subsets and the target is always Dusk/Dawn of BDD100K.

Setting	Source	Method	Person	Car	Rider	Truck	Motor	Bicycle	Bike	mAP
Lower Bound	C	Source Only	26.9	44.7	22.1	17.4	17.1	18.8	16.7	23.4
Lower Bound	C+M	Source Only	35.2	49.5	26.1	25.8	18.9	26.1	26.5	29.7
UDA		UMT [10]	30.7	28.0	3.9	11.2	19.2	17.8	18.7	18.5
UDA		Adaptive Teacher [16]	31.2	31.7	15.1	16.4	17.1	20.9	27.9	22.9
MSDA		TRKP [32]	39.2	53.2	32.4	28.7	25.5	31.1	37.4	35.3
MSDA		PMT [3]	41.1	53.5	31.2	31.9	33.7	34.9	44.6	38.7
MSDA		ACIA(ours)	43.3	58.1	33.3	35.1	33.7	38.6	45.2	41.0
Upper Bound		All-Combined	40.2	60.1	47.1	60.0	29.2	36.3	56.9	47.1
Upper Bound		Fine-Tuning	44.1	61.4	49.0	61.1	30.8	39.2	58.8	49.2
Lower Bound	C+M+S	Source Only	36.6	49.0	22.8	24.9	26.9	28.4	27.7	30.9
UDA		UMT [10]	32.7	39.6	6.6	21.2	21.3	25.7	28.5	25.1
UDA		Adaptive Teacher [16]	36.3	42.6	19.7	23.4	24.8	27.1	33.2	29.6
MSDA		TRKP [32]	40.2	53.9	31.0	30.8	30.4	34.0	39.3	37.1
MSDA		PMT [3]	43.3	54.1	32.0	32.6	35.1	36.1	44.8	39.7
MSDA		ACIA(ours)	44.9	59.2	33.8	33.5	38.3	39.9	46.5	42.3
Upper Bound		All-Combined	41.7	63.9	49.5	58.1	31.6	39.1	53.5	48.2
Upper Bound		Fine-Tuning	49.2	63.5	56.1	62.6	35.1	43.7	57.2	52.5
Upper Bound	C+M+S	Target Only	35.3	53.9	33.2	46.3	25.6	29.3	46.7	38.6

Table 9: Class-wise AP of ACIA compared against the baselines in the mixed adaptation settings. Source domains are Cityscapes(C), MS COCO(M), and Synscapes(S) datasets while the Daytime domain of BDD100K is the target domain.



(a) No class-wise

(b) Prototype based

(c) Ours

Fig. 6: Comparison of instance-level adaptation detection on BDD100k cross-time setting. (a) MSDA without class-conditioned instance adaptation as in [32, 35]. (b) With the prototype-based class-conditional adaptation [3]. (c) ODs with our ACIA approach.